ACS APPLIED MATERIALS & INTERFACES

Research Article

www.acsami.org

Photoinduced Anisotropic Assembly of Conjugated Polymers in Insulating Polymer Blends

Mincheol Chang,[†] Dalsu Choi,[†] Gang Wang,[†] Nabil Kleinhenz,[‡] Nils Persson,[†] Byoungnam Park,[∥] and Elsa Reichmanis*[,†,‡,§]

[†]School of Chemical and Biomolecular Engineering, [‡]School of Chemistry and Biochemistry, and [§]School of Materials Science and Engineering, Georgia Institute of Technology, Atlanta, Georgia 30332-0100, United States

[∥]Department of Materials Science and Engineering, Hongik University, Seoul, 121-791, Korea

Supporting Information

ABSTRACT: Low-dose UV irradiation of poly(3-hexylthiophene) (P3HT)-insulating polymer (polystyrene (PS) or polyisobutylene (PIB)) blend solutions led to the formation of highly ordered P3HT nanofibrillar structures in solidified thin films. The P3HT nanofibers were effectively interconnected through P3HT islands phase-separated from insulating polymer regions in blend films comprising a relatively low fraction of P3HT. Films prepared with a P3HT content as low as 5 wt % exhibited excellent macroscopic charge transport characteristics. The impact of PS on P3HT intramolecular and intermolecular interactions was systematically investigated. The presence of PS chains appeared to assist in the UV irradiation process of the blend solutions to facilitate molecular interactions of the semiconductor component, and to enhance P3HT chain interactions during spin coating because of relatively unfavorable P3HT−PS chain interactions. However, P3HT lamellar packing was hindered in the presence of PS chains, because of favorable hydrophobic interactions between the P3HT hexyl substituents and the PS chains. As a result, the lamellar packing *d*-spacing increased, and the coherence length corresponding to the lamellar packing decreased, as the amount of PS in the blend films increased.

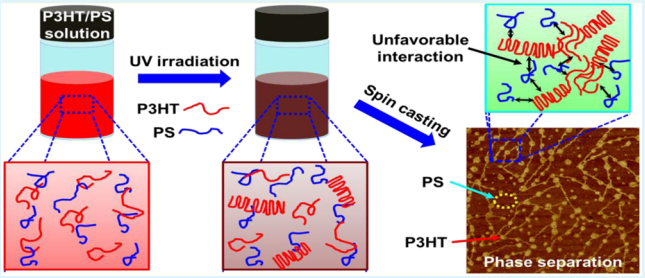

KEYWORDS: *poly(3-hexylthiophene), semiconductor−insulator polymer blends, anisotropic assembly, organic field effect transistors, phase-separation*

1. INTRODUCTION

The use of conjugated polymer semiconductors in organic field-effect transistor (OFET) applications has been extensively investigated, because of their low-temperature, solution-based processability suitable for low-cost, large-area electronic device fabrication.[1−5] However, polymer semiconductor-based devices often suffer from poor environmental stability, which is generally attributed to factors such as molecular structure, chemical impurities, ionization potential, broken conjugation, and/or exposure to oxygen, water, or light.[3,6−11] Typically, high off-currents, large and unstable onset voltages, and large subthreshold slopes result from exposure of OFET devices to the environment.[3,6−11]

Several strategies to overcome degradation of device performance due to environmental exposure have been suggested, including the use of conjugated polymer semiconductor/insulating polymer blends. This solution-based processing approach has been explored because it may provide reduced cost and enhanced mechanical properties, coupled with improved environmental stability for the blend-film-based OFETs.[3,6−8,10,12] However, incorporation of insulating polymers into the OFET active layer may in and of itself lead to a degradation in device performance through dilution of the current density.[7−9,13]

To improve semiconducting chain connectivity and thereby induce more effective charge transport characteristics of the semiconducting layer in the presence of insulating polymers, vertical phase separation between the two polymer components has been induced during film formation by either spin casting or drop casting.[6,8,14] However, vertical phase separation only occurs under limited conditions; the final morphology of the blend films is highly sensitive to many factors including solvent evaporation rate, solubility parameters, film−substrate and film−ambient interactions, surface tension of the components and film thickness.[6,8,14]

Recently, it was shown that nanofibrillar structures of regioregular poly(3-hexylthiophene) (P3HT) provide for sufficient connectivity within an insulating polymer matrix at relatively low semiconductor concentration (ca. 3−20 wt %), to afford mobilities that are comparable to parent 100% P3HT

Received: April 16, 2015
Accepted: June 5, 2015
Published: June 5, 2015

DOI: 10.1021/acsami.5b03310
ACS Appl. Mater. Interfaces 2015, 7, 14095−14103

devices.[3,7,12,15] The nanofibers are generally formed using either a marginal solvent approach or a solvent mixture (lower boiling good solvent/higher boiling poor solvent); inherent solvent characteristics change from "good" to "poor" as the solution temperature decreases or the fraction of poor solvent increases during thin-film formation, which promotes semiconducting polymer chain self-assembly into crystalline nanofibrillar structures through an order−disorder transition of the chains.[7,12,16,17]

However, as polymer regioregularity (RR) and/or MW increases, it becomes difficult to completely dissolve the semiconductor in a marginal solvent even at higher temperatures;[18−22] and it is these high RR and MW polymers that are more desirable for optoelectronic applications, because of their improved electrical properties.[20,22−24] The approach using good/poor solvent mixtures requires substantial optimization to determine the appropriate mixed-solvent composition for a given polymer semiconductor (i.e., different RR or MW) in order to maximize performance. In addition, the above approaches do not provide sufficient time for favorable polymer chain self-assembly; solvent characteristics can quickly change from "good" to "poor", because of decreased temperature or changes in the ratio between solvents in a mixed solvent approach due to rapid film solidification during processing. Consequently, it is difficult to fully maximize the charge transport characteristics of resultant films. Thus, while challenging, it is still desirable to develop a more facile and effective strategy for realizing high-performance, low-cost semiconductor/insulator polymer blend electronic devices.

Generally, semiconducting polymer charge transport characteristics are profoundly affected by polymer chain molecular ordering and thin-film morphology,[20,25,26] and the impact of solvent−polymer and polymer−polymer interactions on the macroscale morphology of polymer blend films has been investigated.[6−8,14,27,28] However, to the best of our knowledge, there have been no systematic studies concerning how those interactions impact polymer semiconductor molecular ordering in blend films.

Here, we demonstrate that ultraviolet (UV) irradiation of polymer semiconductor/insulating polymer solutions is a facile, effective alternative to achieve high-performance, low-cost semiconductor/insulator polymer blends for device applications. P3HT nanofibrillar structures with a high degree of molecular ordering were formed in solutions containing the semiconductor and an insulating polymer through low intensity, limited duration UV irradiation. As a consequence, P3HT islands, which are indicative of phase separation between the two components and generally discontinuous at relatively low semiconductor content, were revealed to be connected through nanofibrillar P3HT aggregates embedded in the insulator matrix. Excellent charge transport was observed from resultant thin films. The impact of insulating polymers on P3HT molecular ordering, morphology, and electrical performance was investigated using static absorption spectroscopy, X-ray diffraction (XRD), atomic force microscopy (AFM), and macroscale charge carrier mobility measurements, as a function of blend composition.

2. RESULTS AND DISCUSSION

P3HT was blended with amorphous polystyrene (PS), a common insulating polymer, to fabricate semiconductor/insulator polymer blend OFET devices.[3,7] Figure 1 presents a schematic illustration of the photoinduced anisotropic assembly

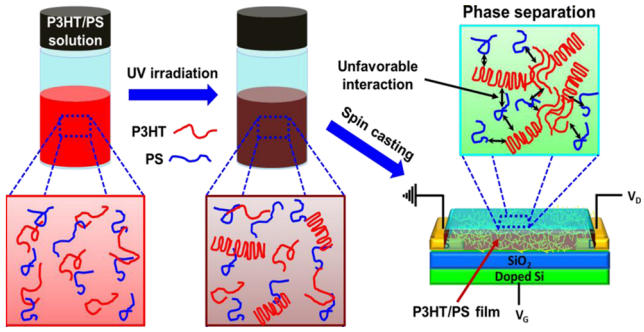

Figure 1. Schematic illustration of the procedure for fabricating a field-effect transistor based on a P3HT/PS blend film.

of P3HT chains and subsequent fabrication process for corresponding thin-film-based transistors. In a typical experiment, defined quantities of P3HT/$CHCl_3$ and PS/$CHCl_3$ solutions were mixed in a 20 mL borosilicate glass vial, and then exposed to low-intensity, limited-duration UV radiation. As reported previously, the process caused no discernible degradation of P3HT.[20] The semiconducting polymer chains self-assembled into fibrillar aggregates via main chain conformational changes from aromatic to quinoid-like structure under UV irradiation. Photoexcitation is well-known to afford charge injection into conjugated polymers such as polythienylenes, resulting in local structural distortion and the formation of self-localized polarons or bipolarons with associated electronic states in the energy gap.[29] In the ground state, the conjugated P3HT segments are largely aromatic in character, whereas, upon photoexcitation, the nuclear geometry of the segments rearranges into a more stable configuration (i.e., quinoid character).[20,29−31] The quinoid structure has higher degree of coplanarity, facilitating more favorable $\pi-\pi$ interchain interactions.[30,31] The aggregates formed in solution via UV treatment survive a spin-coating process and appear as nanofibrillar structures in resultant P3HT/PS blend thin films.

AFM studies were performed to investigate the morphology of P3HT/PS blend films with different fractions of P3HT. Figure 2a shows the changes in blend thin-film surface morphology of either nonirradiated or UV-irradiated polymer solutions after thin-film deposition. The optimized UV irradiation time was defined as the time when the P3HT films underwent no additional changes in morphology. This time was consistent with previously reported results for UV irradiation of pristine P3HT solutions.[20] In order to minimize use of the relatively high cost semiconductor and concomitantly improve passivation, relatively higher proportions of PS (>50 wt %) were blended with P3HT. In the absence of UV exposure, bare P3HT films appear featureless and amorphous-like, while blend films show two distinct phases: light and dark. The light features decrease as the P3HT content decreases, suggesting that these regions correspond to the semiconductor phase. Typically, for the ratios investigated here, P3HT forms isolated, spherical, cluster-like features in the P3HT/PS blends when spin-coated from the corresponding $CHCl_3$ solutions.[7,15,28]

Phase separation in polymer blend films is dependent on molecular (i.e., polymer solubility, miscibility of two polymers, surface energy of substrate, and volatility, viscosity, and surface tension of solvent), thermodynamic (i.e., composition, temperature, and pressure) and processing parameters (i.e., film deposition method).[6,8,27,32] Generally, the effect of polymer

DOI: 10.1021/acsami.5b03310
ACS Appl. Mater. Interfaces 2015, 7, 14095−14103

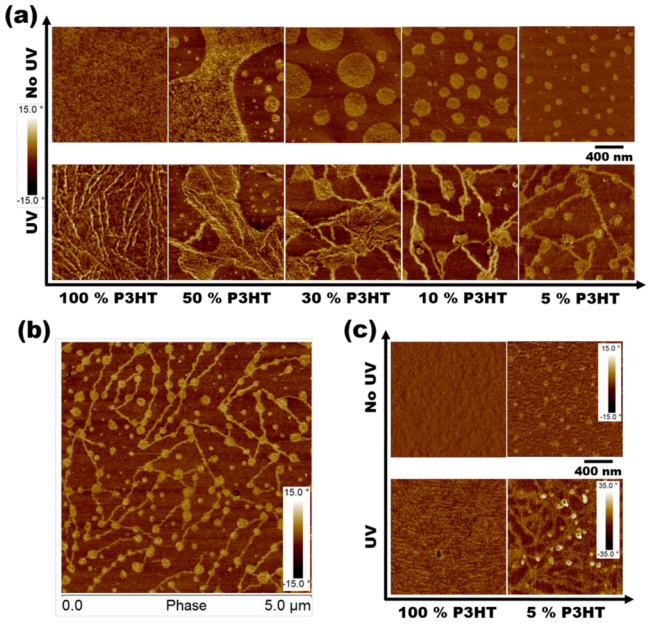

Figure 2. (a) Tapping-mode AFM phase images of the top surface of P3HT/PS blend films spin-coated from pristine and 8-min UV-treated blend solutions, respectively. (b) Overview (5 μm × 5 μm) of top surface of P3HT/PS blend film obtained from 8-min UV-treated blend solution with 5 wt % P3HT. (c) AFM phase images of bottom surface of pure P3HT and P3HT/PS (5/95) blend films spin-coated from corresponding pristine and UV-treated solutions, respectively.

solubility has been widely taken into account to understand the phase separation of polymer blends during a spin-coating process.[27,31] It has been suggested that, during spin-casting, a PS-top/P3HT-bottom bilayer (vertical phase separation) is transiently formed when dewetting is negligible; P3HT ($\delta \approx 14.8$ MPa$^{1/2}$)[33] is depleted more quickly (not completely) from solution, because of lower solubility than PS ($\delta \approx 17.9$ MPa$^{1/2}$)[33] in $CHCl_3$ ($\delta \approx 19$ MPa$^{1/2}$)[1] and deposited on the SiO_2 substrate, while PS tends to remain in the liquid phase and thereby, is enriched at the surface.[27] However, the bilayer structure becomes fragmented by a Marangoni-like instability at the polymer/polymer interface, and thereby finally adopts a laterally phase-separated structure when the film thickness decreases below a certain critical value;[27,34] PS ($\gamma \approx 40.2$ mJ/m^2)[35] will tend to migrate toward the SiO_2 ($\gamma \approx 36.5$ mJ/m^2) substrate,[27] while P3HT ($\gamma \approx 21.0$ mJ/m^2)[36] is likely to migrate to the air/film interface for energy minimization. It is believed that voids form in the upper PS-rich solution layer, which become filled with the lower, P3HT-rich liquid phase.[37]

In contrast to the blend films spin-coated from the untreated solutions, those obtained from UV-irradiated solutions exhibit three apparently different parts, featureless, island-like, and nanofibrillar (Figure 2a). P3HT nanofibers formed in the blend solutions via UV irradiation appear to interconnect P3HT islands in the UV-treated films, and those islands decrease in size with decreased proportions of P3HT. Interestingly, good interconnectivity of the P3HT domains continues to be observed as P3HT blend content decreases to 5 wt % (Figure 2b).

Since it is the substrate/polymer interface that is important in charge transport for bottom-gate/bottom-contact OFET devices, the bottom surface morphology was also investigated using literature methodologies.[12] (See the Supporting Information of ref 12). To peel the films from the SiO_2 substrate, they were covered with an epoxy resin, and then immersed in liquid nitrogen. As shown in Figure 2c, 100% P3HT and P3HT/PS (5/95) blend films obtained from both untreated and 8-min UV-treated solutions exhibit similar bottom and top surface morphologies. P3HT islands dominate the top surface of both blend films because P3HT-rich solution is likely to migrate to the air/film interface (*vide supra*), filling voids formed in the upper PS-rich solution layer. Significantly, the density of P3HT nanofibrillar structures is noticeably higher at the bottom surface of both UV-treated solutions; the aggregated P3HT component is likely to precipitate at the bottom surface during spin coating, perhaps because of gravitational forces.[30]

Blend film morphology was also interrogated using polarized optical microscopy (POM), as seen in Figure 3. While the film

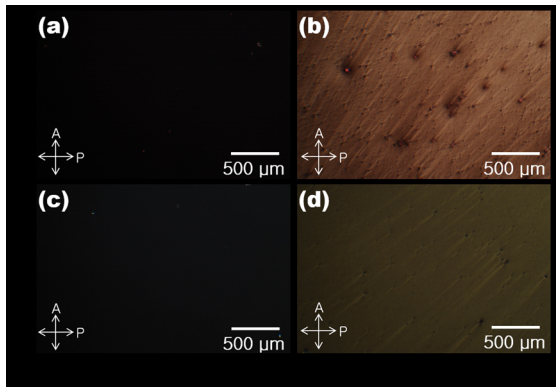

Figure 3. Polarized optical microscopy (POM) images of thin films spin-coated on glass from $CHCl_3$ solutions of (a) pristine P3HT, (b) UV-irradiated P3HT, (c) pristine P3HT/PS (30/70) blend, and (d) UV-irradiated P3HT/PS (30/70) blend. All images are taken with crossed polarizers.

obtained from the untreated 100% P3HT solution appears dark (isotropic), that from UV-irradiated P3HT solution appears bright under crossed polarizers, suggesting that the film is anisotropic and birefringent. Films obtained from nonirradiated and UV-irradiated P3HT/PS (30/70) blend solutions exhibit comparable, although somewhat less distinct results relative to their pristine counterparts. Specifically, the irradiated sample displays birefringent textures indicative of enhanced polymer thin-film ordering or crystallinity.[20] These observations suggest that the UV irradiation process affords highly ordered P3HT aggregates, even in the presence of inert components such as PS. It should be noted that birefringent textures are barely visible in films spin-coated from UV-irradiated solutions of lower P3HT concentration (10 and 5 wt %), because of the highly diluted crystalline P3HT regions in the amorphous PS matrix (see Figure S1 in the Supporting Information).

UV-vis spectroscopy, which provides further insights relating to intermolecular and intramolecular ordering of polymer semiconductor chains, was used to investigate how PS affects P3HT chain aggregation.[20,25,38] Figure 4a presents the spectrum of untreated P3HT/$CHCl_3$, which exhibits only higher-energy features (π–π^* intraband transition) at ~450 nm.[38] The corresponding blend solutions exhibited identical UV-vis spectral features to those of the single component solution; P3HT chains are likely to be fully dissolved, and the presence of PS does not lead to solution-phase P3HT aggregation (data not included). Figure 4b depicts the

DOI: 10.1021/acsami.5b03310
ACS Appl. Mater. Interfaces 2015, 7, 14095−14103

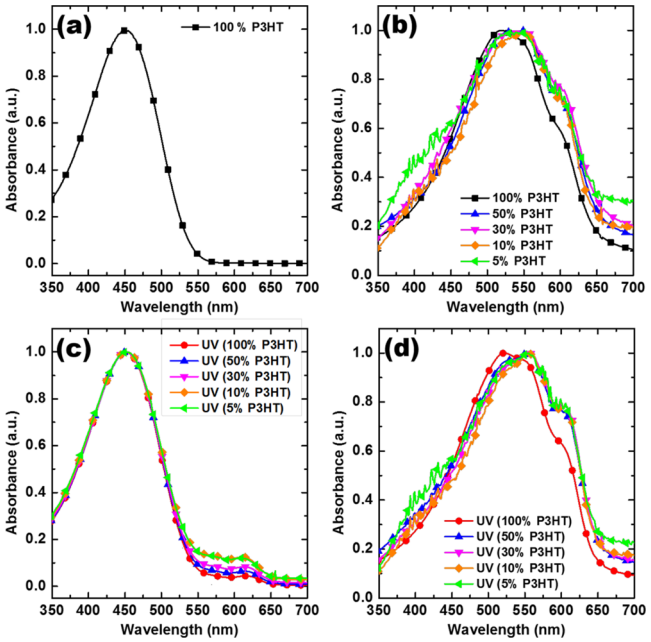

Figure 4. Normalized UV-vis absorption spectra of (a) pristine P3HT solution from $CHCl_3$ and (b) pristine P3HT film and P3HT/PS blend films with different weight ratios (50/50, 30/70, 10/90, and 5/95), obtained by spin coating. Normalized UV-vis absorption spectra of (c) UV-irradiated pure P3HT solution and UV-irradiated P3HT/PS (50/50, 30/70, 10/90, and 5/95) blend solutions from $CHCl_3$ and (d) corresponding films.

electronic absorption spectra of the blend films spin-coated from the respective nonirradiated P3HT/PS solutions. Although the spectral intensity degrades with increased PS content, because of dilution effects, the lower-energy features (~555 and 605 nm) associated with interchain coupling are clearly more enhanced, suggesting that PS chains facilitate P3HT chain aggregation (intermolecular $\pi-\pi$ interaction) during spin coating.[20,25] As $CHCl_3$ evaporates, the relatively unfavorable interactions between P3HT and PS become dominant, which enables P3HT aggregation via favorable $\pi-\pi$ interactions between semiconducting polymer chains.[28] It could be anticipated that the islands of P3HT formed in the blend films have a higher degree of molecular ordering, compared to the pure P3HT sample.

In contrast to the untreated solutions, as seen from Figure 4c upon UV exposure for 8-min lower-energy features (~570 and 620 nm) appear and increase in intensity as PS content increases. In the absence of UV treatment, unfavorable P3HT-PS interactions did not promote P3HT chain aggregation, because favorable P3HT-$CHCl_3$ and PS-$CHCl_3$ interactions are dominant. However, upon UV irradiation, the presence of PS appears to assist in P3HT aggregation, perhaps as a result of those same relatively unfavorable P3HT-PS interactions. Films obtained from the UV-irradiated solutions (Figure 4d) exhibited more-enhanced low-energy features (~555 nm (0–1) and 605 nm (0–0)) than their untreated counterparts, indicating that the aggregates formed upon irradiation survive the rapid thin-film deposition process, and then coexist with the aggregates formed during deposition.

UV-vis absorption spectroscopy and quantitative modeling allows detailed analysis of P3HT polymer chain intramolecular ordering. The P3HT absorption spectrum comprises two phases: a crystalline region (lower energy) due to ordered chains and an amorphous region (higher energy) due to disordered chains.[38] According to Spano's model, the crystalline regions are assumed to be composed of weakly interacting H-aggregates, which exhibit low-energy features, so-called "vibronic bands", in the absorption spectrum.[38] These vibronic bands can be related to free exciton bandwidth (W), which correlates with intramolecular ordering (conjugation length) of an individual polymer chain.[20,38,39] A decrease in W indicates an increase in both average intramolecular ordering and conjugation length of an individual polymer chain in the aggregates.[20,38,39] The W values are calculated using eq 1 and the intensities of the (0–0) and (0–1) transitions obtained from Gaussian fits to the experimental spectra (see Figures S2–S4 in the Supporting Information).[38]

$$\frac{I_{0-0}}{I_{0-1}} \approx \left(\frac{1 - 0.24W/E_p}{1 + 0.073W/E_p}\right)^2 \quad (1)$$

I_{0-0} and I_{0-1} represent the intensities of the (0–0) and (0–1) transitions, respectively and E_p is the vibrational energy of the symmetric vinyl stretch (taken as 0.18 eV).[38] W values for the nonirradiated solutions could not be calculated, because no aggregates formed in solution. As shown in Figure 5a, the W

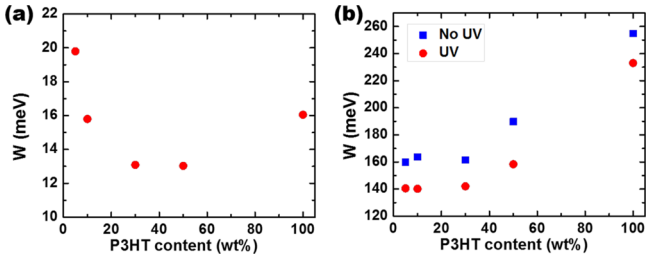

Figure 5. Evolution of exciton bandwidth (W) of (a) P3HT/PS blend solutions treated by UV irradiation for 8 min and of (b) pristine P3HT/PS blend films and P3HT/PS blend films spin-coated from 8-min UV-irradiated blend solutions. The P3HT content of the blend films: 5, 10, 30, 50, and 100 wt %.

value for aggregates formed in the UV-treated solutions does not significantly change (Figure 5b); the value slightly decreases from ~16 meV to 13 meV as the PS content increases from 0 to 70 wt %, and then increases up to ~20 meV with further increases in PS up to 95 wt %. Thus, the presence of PS has only a limited effect on P3HT aggregate intramolecular ordering in blend solutions during UV irradiation. Conceivably, because of relatively unfavorable interactions between P3HT and PS during film formation, films obtained from untreated blend solutions exhibited enhanced P3HT intramolecular ordering with increased levels of PS; the W value for P3HT within the nonirradiated samples decreased from 255 meV to 160 meV with increased PS content up to 70 wt %, and then saturated as the proportion of PS further increased to 95 wt %. P3HT main chains become planarized during film formation to decrease their energy, i.e., the effective conjugation length of the main chains is increased, which is indicative of enhanced intramolecular interactions of the semiconducting chains. The value of W for P3HT embedded within films obtained from the corresponding UV-treated solutions varied in a manner similar to that for the nonirradiated counterparts, as shown from Figure 5b. However, the blend films obtained from UV-irradiated solutions exhibited relatively more-enhanced intramolecular interactions; W

DOI: 10.1021/acsami.5b03310
ACS Appl. Mater. Interfaces 2015, 7, 14095–14103

gradually decreased from 233 meV to 140 meV with increasing levels PS content (0 to 70 wt %), and then saturated with further increases in PS. While scattering effects from polycrystalline P3HT led to a shift in baseline for the solidified film spectra, the magnitude may impact the quantitative W values but not the observed trends.

The effect of PS on P3HT microstructure (crystallinity and lamellar packing) was also investigated. For the untreated blend films, the (100) peak intensity, which is associated with polymer chain lamellar packing along the crystallographic direction perpendicular to the backbone, appeared too weak to calculate either d-spacing or crystal grain size, particularly at low P3HT concentrations (<30 wt %) (data not included). Figure 6a presents X-ray diffractograms obtained from grazing-

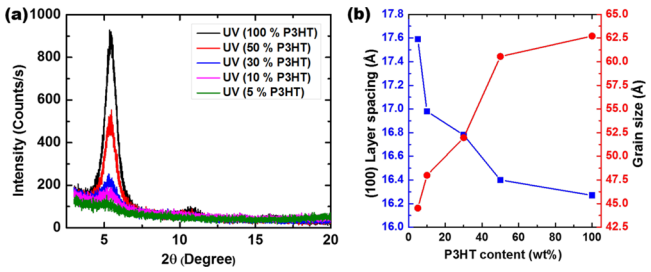

Figure 6. (a) GIXRD profiles of P3HT/PS blend films obtained from the UV irradiated corresponding blend solutions and (b) (100) layer spacing (left axis) and crystal grain size along the [100] direction, calculated from corresponding GIXRD data.

incidence X-ray diffraction (GIXRD) measurements of films obtained from spin-coated UV-irradiated blend solutions. Although these films exhibited increased intramolecular and intermolecular P3HT chain ordering with increased PS content, the intensity of the (100) peak decreased as the PS increased, simply because PS dilutes the concentration of P3HT in the blends. Also, a (100) peak shift to lower angle, from 5.4° to 5.0°, is observed as the PS content increases from 0 to 95 wt %, indicative of an increase in d-spacing in the direction along the side chains, parallel to the polymer main chain, from 16.3 Å to 17.6 Å. These results suggest that the extent of interdigitation between P3HT alkyl side chains decreased as the levels of PS increased, perhaps because of favorable hydrophobic interactions between the hexyl substituents and the PS chains,[40] which might attenuate the interactions between hexyl groups. Concomitantly, interactions between the polythiophene (PT) main chain might be expected to increase via favorable $\pi-\pi$ interactions, facilitated by relatively unfavorable interactions between PT and PS. In addition, the presence of PS chains impacted the coherence length corresponding to P3HT lamellar packing along the [100] direction, as calculated using Scherrer's relation:[26,28]

$$D_{hkl} = \frac{0.9\lambda}{\beta_{hkl} \cos\theta} \quad (2)$$

where D_{hkl} is the apparent crystal size along the [hkl] direction, λ is the X-ray wavelength, and β_{hkl} is the full width at half-maximum of a (hkl) diffraction (in radians). Scherrer analysis of the diffraction peaks reveals that the coherence length (grain size) corresponding to the interlayer packing along the [100] direction decreases from 6.3 nm to 4.5 nm as the PS content increased from 0 to 95 wt %. Conceivably, as the PS content increases, P3HT chain aggregation is facilitated in order to minimize relatively unfavorable P3HT−PS chain interactions during the UV irradiation and/or spin-casting processes. Rapid aggregation of the polymer chains is expected to hinder further/continued growth of the polymer crystallites.[26] In addition, favorable hydrophobic interactions between the hexyl moieties and the PS chains would hinder growth of P3HT crystallites along the [100] direction, attenuating interactions (lamellar packing) between hexyl side chains.

To investigate the electrical performance of resultant films, bottom-gate bottom-contact OFET devices were fabricated by spin-coating the respective blend solutions onto device substrates (transistor channel width = 2000 μm and length = 50 μm). Figure 7a depicts the mobility of the resultant films

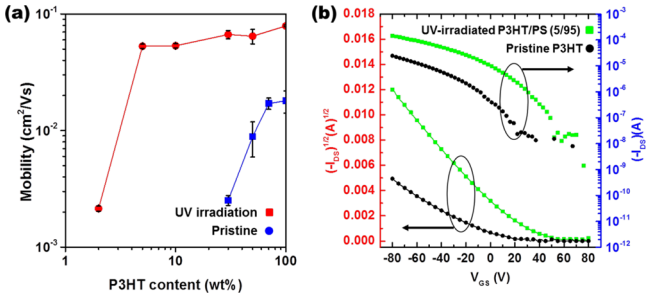

Figure 7. (a) Average field-effect mobilities of pristine P3HT/PS (30/70, 50/50, 70/30, 100/0) blend films and P3HT/PS (2/98, 5/95, 10/90, 30/70, 50/50, and 100/0) blend films spin-coated from 8-min UV-irradiated blend solutions. (b) Transfer characteristics of devices based on pristine P3HT and P3HT/PS (5/95) blend film obtained from 8-min UV-irradiated corresponding solutions, respectively. Mobilities were calculated in the saturation regime of operation with V_{DS} = −80 V.

obtained from untreated blend solutions and the corresponding UV-treated solutions. The films obtained via UV treatment exhibit consistently higher mobilities, most likely due to the presence of highly ordered P3HT fibrillar structures formed upon UV irradiation. The mobility of untreated samples decreased dramatically from 1.80×10^{-2} cm^2 V^{-1} s^{-1} to 2.5×10^{-3} cm^2 V^{-1} s^{-1} as the PS content increased from 0 to 70 wt %, and was not detected at P3HT concentrations below 30 wt %. In contrast, when irradiated solutions were used to fabricate devices, even when P3HT concentration decreased to 5 wt %, the films continued to exhibit mobilities (~5.3×10^{-2} cm^2 V^{-1} s^{-1}) comparable to that for 100% P3HT (~7.9×10^{-2} cm^2 V^{-1} s^{-1}). Note that the effective channel width (W) for the 5 wt % P3HT blend film is substantially smaller than that for 100% P3HT; however, channel length (L) is essentially unchanged. Thus, the calculated mobility for the 5 wt % P3HT devices may be viewed as a lower bound. Significantly, even devices fabricated with irradiated 5 wt % P3HT solutions displayed mobilities even higher than that determined for untreated, 100% P3HT (~1.80×10^{-2} cm^2 V^{-1} s^{-1}).

The macroscopic charge transport results agree well with AFM analysis of the blend films (Figure 2). As PS content increases, the P3HT phase in the untreated blend films becomes discontinuous, whereas the blend films obtained from UV-treated solutions exhibit excellent interconnectivity between P3HT regions, which is ascribed to the presence of P3HT nanofibrillar structures. As P3HT content was decreased further to 2 wt %, the thin-film macroscopic mobility dramatically decreased to ~2.1×10^{-3} cm^2 V^{-1} s^{-1}. Figure 7b depicts transfer curves for OFET devices fabricated from

DOI: 10.1021/acsami.5b03310
ACS Appl. Mater. Interfaces 2015, 7, 14095−14103

untreated P3HT and 8-min UV-irradiated P3HT/PS (5/95) films, which are typical of p-channel OFET operation in the accumulation mode. The saturation drain current (I_{DS}) is recorded as ~2.4 × 10^{-5} A for the P3HT FET; while it is ~6 times higher for the latter (~1.4 × 10^{-4} A), because of the formation of P3HT fibrillar structures, which serve to form interconnection pathways within the film. The blend-film-based OFET device exhibited a turn-on voltage (V_{ON}) higher than that of the pristine device, which is attributed to the effects of additional doping and/or charge trapping at grain boundaries/interfaces.[20,25,41,42]

For any targeted application, OFET ambient stability is critical. Encapsulation of the active semiconductor with an insulating polymer layer has proven effective for improving long-term device stability. Figure 8a presents the change in current on/off ratio for transistors fabricated from UV-treated P3HT/PS solutions upon exposure to air. The transistors exhibited an on/off ratio of ~10^4, regardless of P3HT/PS ratio, when tested immediately after device fabrication. However, after air exposure for 7 days, the ratio decreased: the decrease was more significant with increased proportions of P3HT. The P3HT/PS (5/95) device current on/off ratio decreased to ~10^3, whereas, for 100% P3HT devices, the value decreased to considerably less than 10^2. These results suggest that PS may inhibit the penetration of air into embedded P3HT regions. Note that PS is not a particularly good oxygen barrier, because of its lack of polar side groups.[10] After exposure to air for 7 days, the on-current barely changed while the off-current significantly increased as the PS content decreased, as shown in Figures 8b and 8c, as well as Figure S5 in the Supporting Information. The increased off-current is attributable to oxygen doping that increases the bulk conductivity of the films.[3,10,43]

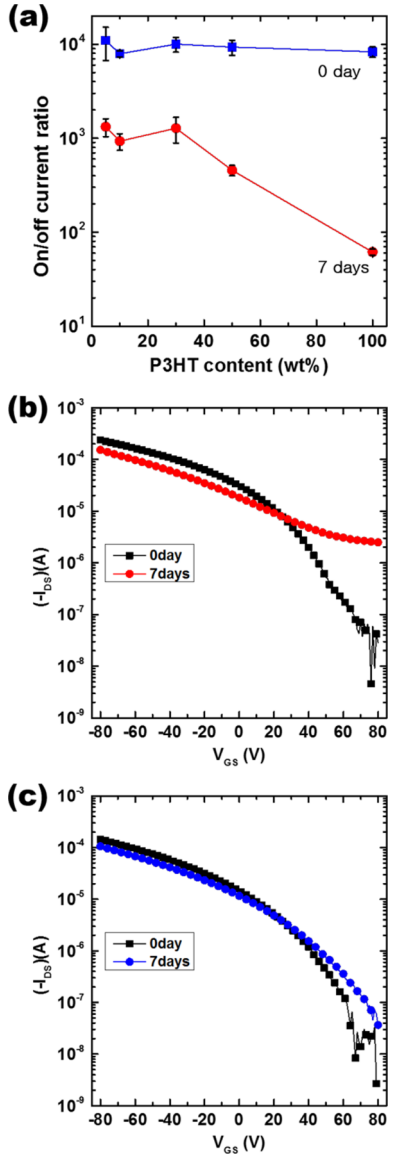

Figure 8. (a) Average on/off current ratio of the devices based on P3HT/PS blend films before and after exposure to air for 7 days. Transfer characteristics of devices based on (b) homo P3HT and (c) P3HT/PS (5/95) blend film before and after exposure to air for 7 days. All films were spin-coated from their corresponding solutions treated by UV irradiation for 8 min.

UV irradiation was also found to facilitate the molecular assembly of P3HT into long fibrillar structures in an alternate blend solution, P3HT/PIB (polyisobutylene). As in the case of PS, UV irradiation of PIB blend solutions led to the formation of P3HT fibrillar structures, which served to connect isolated P3HT islands within the corresponding films (see Figures 9a and 9b). Consequently, as shown in Figure 9c, the P3HT/PIB blend films spin-coated from the corresponding UV-irradiated solutions exhibited higher mobility than 100% P3HT films prepared from untreated solutions, even as the P3HT content decreased to 10 wt % (2.3 × 10^{-2} cm^2 V^{-1} s^{-1} for P3HT/PIB (10/90) vs 1.8 × 10^{-2} cm^2 V^{-1} s^{-1} for 100% P3HT).

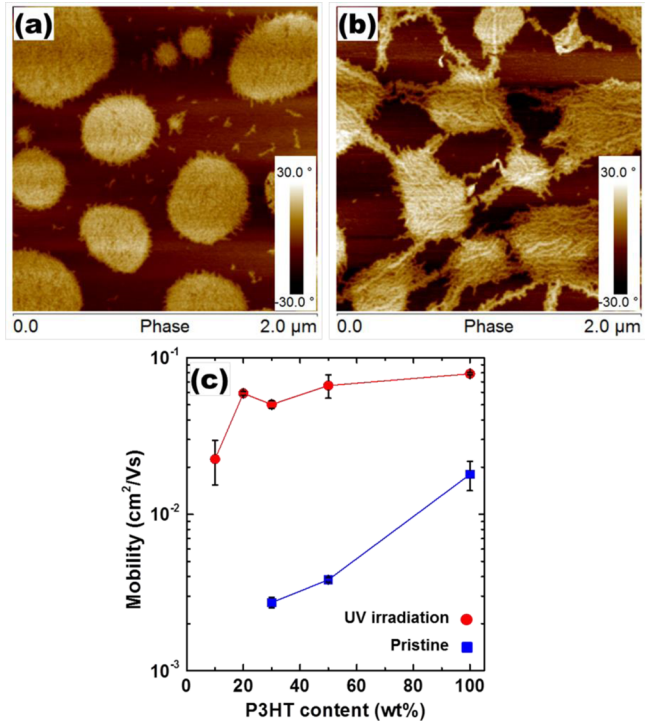

Figure 9. Tapping-mode AFM phase images of P3HT/PIB (30/70) blend films spin-coated from (a) pristine blend solution and (b) 8-min UV-treated blend solution, respectively. (c) Average field-effect mobilities of pristine P3HT/PIB blend (30/70, 50/50, and 100/0) films and P3HT/PIB (10/90, 20/80, 30/70, 50/50, and 100/0) blend films spin-coated from 8-min UV-irradiated blend solutions.

DOI: 10.1021/acsami.5b03310
ACS Appl. Mater. Interfaces 2015, 7, 14095−14103

3. CONCLUSIONS

In conclusion, this work demonstrates that low-dose UV irradiation of polymer semiconductor/insulating polymer solutions is a facile, effective alternative processing method to achieve high-performance, low-cost semiconductor/insulator polymer-blend-based transistor devices. Highly ordered P3HT nanofibrillar structures were formed in P3HT/PS blend solutions upon exposure to low doses of UV irradiation. Within films prepared from the irradiated solutions, P3HT islands isolated from PS-rich regions were effectively connected by P3HT nanofibrillar aggregates within the blend films, resulting in excellent charge transport characteristics, even at P3HT content as low as 5 wt %. Furthermore, the PS layer provided for improved ambient stability.

The impact of PS on intramolecular and intermolecular P3HT chain interactions was systematically investigated. PS chains assisted the UV-assisted aggregation process in blend solution, and enhanced intramolecular and intermolecular P3HT chain interactions during active layer deposition via relatively unfavorable interactions between the two polymer components. However, PS appeared to hinder the lamellar packing between P3HT chains, likely because of favorable hydrophobic interactions between the hexyl side chains and PS chains, resulting in an increase in the lamellar packing *d*-spacing and decrease in the coherence length, corresponding to lamellar packing.

These results demonstrate the viability of UV-assisted conjugated polymer aggregation as a technique to promote macroscopic charge carrier transport in semiconductor−insulator polymer blend films. The formation of nanofibrillar aggregates in polymer blend solutions where the active component is <10 wt % of the total solids content is sufficient to provide for effective interconnection pathways between phase-separated semiconducting polymer domains within blend films. The process presented here may facilitate development of active layer formulations suitable for the fabrication of large-area, flexible organic electronics having low cost, high environmental stability, and good mechanical properties.

4. MATERIALS AND METHODS

Materials. Regioregular P3HT (M_w of 43.7 kDa and M_n of 19.7 kDa) was purchased from Rieke Metals, Inc., and used without further purification. Amorphous PS (M_w of 350 kDa and M_n of 170 kDa) and chloroform (anhydrous grade) were purchased from Sigma−Aldrich, and used without further purification. The head-to-tail regioregularity (RR) of P3HT was estimated to be ∼96% from the ^{1}H NMR spectra obtained from deuterated chloroform solution at 293 K using a Bruker DSX 300.

Anisotropic Growth of P3HT Aggregates in the Solution. Twenty milligrams (20 mg) of P3HT/PS with relevant ratio was introduced into 2 mL of chloroform in a 20 mL borosilicate glass vial in air. Subsequently, the vial was sealed with a cap and the solution was stirred for at least 60 min at ∼55 °C to completely dissolve the polymer. The as-prepared solution was cooled to ambient temperature, and, in turn, the solution was treated by UV irradiation. To conduct UV irradiation of the solution, the vial containing the solution was placed on a hand-held UV lamp (Entela, Model UVGL-15, 5 mW cm^{-2}, 254 nm) which had been placed on a magnetic stirrer (Corning, Inc.). The solution then was gently stirred and irradiated using the lamp for 8 min. The irradiation was performed through the bottom wall of the borosilicate glass vial, which transmits more than 90% of the incident 254 nm light.

Organic Field-Effect Transistor (OFET) Fabrication and Characterization. The OFET devices used for electrical characterization consisted of two contact devices, where P3HT/PS blend films were deposited by spin-coating the relevant polymer solutions onto a 300-nm-thick SiO_2 gate dielectric. The highly doped substrate wafer served as the gate electrode, while Au/Cr was used for the source and drain contacts. The source and drain contacts were fabricated using a standard photolithography based lift-off process, followed by E-beam evaporation (Denton Explorer) of 50 nm Au contacts with 3 nm of Cr as the adhesion layer. Before spin-coating P3HT/PS blend solutions, all devices were cleaned for 15 min in a UV-ozone cleaner (Novascan PSD-UV) to completely remove any residual photoresist and other organic contaminants. OFET devices were prepared by spin-coating (WS-650MZ-23NPP, Laurell) the solutions onto precleaned substrates at a spin speed of 1500 rpm for 60 s in air, and tested in nitrogen ambient using an Agilent Model 4155C semiconductor parameter analyzer. The P3HT/PS blend films obtained by spin-coating were found to have a thickness in the range of 66−96 nm, as measured by a profilometer (Veeco Instruments, Inc., Model Dektak 3030). The devices were stored in a vacuum oven (1 Torr) overnight at room temperature to remove residual solvent. The field-effect mobility was calculated in the saturation regime of transistor operation (V_{DS} = −80 V) by plotting the drain current (I_{DS}) versus gate voltage (V_{GS}) and fitting the data to the following equation:

$$I_{DS} = \frac{WC_{ox}}{2L}\mu(V_{GS} - V_T)^2 \quad (3)$$

where W (2000 μm) and L (50 μm) are the transistor channel width and length, respectively; V_T is the threshold voltage; and C_{OX} is the capacitance per unit area of the silicon dioxide gate dielectric (1.15 × 10^{-8} F/cm^2).

UV-vis Spectroscopy. The solution and solid-state UV-vis spectra were recorded using an Agilent Model 8510 UV-vis spectrometer. Films for solid-state studies were prepared by spin-coating the requisite solution onto precleaned glass slides following the same procedures used to prepare OFET devices.

Grazing Incidence X-ray Diffraction (GIXRD). Out-of-plane grazing-incidence X-ray diffraction data were obtained using a Panalytical X'Pert Pro system equipped with a Cu X-ray source operating at 45 kV and 40 mA. The grazing-incidence angle was fixed at 0.2°, and the detector was scanned from 3° to 20°.

Atomic Force Microscopy (AFM). The AFM measurements were performed on films spin-coated onto bottom contact OFET devices using an ICON dimension scanning probe microscope (Bruker) operating in tapping mode with a silicon tip (RTESP, Bruker).

■ ASSOCIATED CONTENT

Ⓢ Supporting Information

Polarized optical microscopy images of thin films spin-coated on glass from chloroform solutions of UV-irradiated P3HT/PS blends with 10 and 5 wt % P3HT, respectively, the results of fits to UV-vis absorption spectra of the P3HT/PS blend solutions and corresponding films, and on- and off-current of the devices based on P3HT/PS blend films spin coated from corresponding blend solutions treated by UV irradiation for 8 min before and after air exposure for 7 days. The Supporting Information is available free of charge on the ACS Publications website at DOI: 10.1021/acsami.5b03310.

■ AUTHOR INFORMATION

Corresponding Author

*E-mail: ereichmanis@chbe.gatech.edu.

Notes

The authors declare no competing financial interest.

■ ACKNOWLEDGMENTS

The financial support of the Georgia Institute of Technology and the Air Force Office of Scientific Research (No. FA9550-12-1-0248) is gratefully acknowledged. N.P. appreciates

DOI: 10.1021/acsami.5b03310
ACS Appl. Mater. Interfaces 2015, 7, 14095−14103

support from the National Science Foundation IGERT FLAMEL program (Grant No. 1258425, IGERT-CIF21), and G.W. receives support from the China Scholarship Council.

REFERENCES

(1) Chang, M.; Choi, D.; Fu, B.; Reichmanis, E. Solvent Based Hydrogen Bonding: Impact on Poly(3-hexylthiophene) Nanoscale Morphology and Charge Transport Characteristics. *ACS Nano* **2013**, *7*, 5402−5413.
(2) Li, J. H.; Sun, Z. H.; Yan, F. Solution Processable Low-Voltage Organic Thin Film Transistors with High-*K* Relaxor Ferroelectric Polymer as Gate Insulator. *Adv. Mater.* **2012**, *24*, 88−93.
(3) Lu, G. H.; Blakesley, J.; Himmelberger, S.; Pingel, P.; Frisch, J.; Lieberwirth, I.; Salzmann, I.; Oehzelt, M.; Di Pietro, R.; Salleo, A.; Koch, N.; Neher, D. Moderate Doping Leads to High Performance of Semiconductor/Insulator Polymer Blend Transistors. *Nat. Commun.* **2013**, *4*, 1588.
(4) Forrest, S. R. The Path to Ubiquitous and Low-Cost Organic Electronic Appliances on Plastic. *Nature* **2004**, *428*, 911−918.
(5) Yan, H.; Chen, Z. H.; Zheng, Y.; Newman, C.; Quinn, J. R.; Dotz, F.; Kastler, M.; Facchetti, A. A High-Mobility Electron-Transporting Polymer for Printed Transistors. *Nature* **2009**, *457*, 679−686.
(6) Arias, A. C.; Endicott, F.; Street, R. A. Surface-Induced Self-Encapsulation of Polymer Thin-Film Transistors. *Adv. Mater.* **2006**, *18*, 2900−2904.
(7) Qiu, L. Z.; Lee, W. H.; Wang, X. H.; Kim, J. S.; Lim, J. A.; Kwak, D.; Lee, S.; Cho, K. Organic Thin-Film Transistors Based on Polythiophene Nanowires Embedded in Insulating Polymer. *Adv. Mater.* **2009**, *21*, 1349−1353.
(8) Goffri, S.; Muller, C.; Stingelin-Stutzmann, N.; Breiby, D. W.; Radano, C. P.; Andreasen, J. W.; Thompson, R.; Janssen, R. A. J.; Nielsen, M. M.; Smith, P.; Sirringhaus, H. Multicomponent Semiconducting Polymer Systems with Low Crystallization-Induced Percolation Threshold. *Nat. Mater.* **2006**, *5*, 950−956.
(9) Babel, A.; Jenekhe, S. A. Morphology and Field-Effect Mobility of Charge Carriers in Binary Blends of Poly(3-hexylthiophene) with Poly[2-methoxy-5-(2-ethylhexoxy)-1,4-phenylenevinylene] and Polystyrene. *Macromolecules* **2004**, *37*, 9835−9840.
(10) Fu, Y.; Tsai, F. Y. Air-Stable Polymer Organic Thin-Film Transistors by Solution-Processed Encapsulation. *Org. Electron.* **2011**, *12*, 179−184.
(11) Ficker, J.; von Seggern, H.; Rost, H.; Fix, W.; Clemens, W.; McCulloch, I. Influence of Intensive Light Exposure on Polymer Field-Effect Transistors. *Appl. Phys. Lett.* **2004**, *85*, 1377−1379.
(12) Lim, J. A.; Kim, J. H.; Qiu, L.; Lee, W. H.; Lee, H. S.; Kwak, D.; Cho, K. Inkjet-Printed Single-Droplet Organic Transistors Based on Semiconductor Nanowires Embedded in Insulating Polymers. *Adv. Funct. Mater.* **2010**, *20*, 3292−3297.
(13) Liu, J. S.; Sheina, E.; Kowalewski, T.; McCullough, R. D. Tuning the Electrical Conductivity and Self-Assembly of Regioregular Polythiophene by Block Copolymerization: Nanowire Morphologies in New Di- and Triblock Copolymers. *Angew. Chem., Int. Ed.* **2002**, *41*, 329−332.
(14) Qiu, L.; Lim, J. A.; Wang, X.; Lee, W. H.; Hwang, M.; Cho, K. Versatile Use of Vertical-Phase-Separation-Induced Bilayer Structures in Organic Thin-Film Transistors. *Adv. Mater.* **2008**, *20*, 1141−1145.
(15) Lu, G. H.; Tang, H. W.; Qu, Y. P.; Li, L. G.; Yang, X. N. Enhanced Electrical Conductivity of Highly Crystalline Polythiophene/Insulating-Polymer Composite. *Macromolecules* **2007**, *40*, 6579−6584.
(16) Kiriy, N.; Jahne, E.; Adler, H. J.; Schneider, M.; Kiriy, A.; Gorodyska, G.; Minko, S.; Jehnichen, D.; Simon, P.; Fokin, A. A.; Stamm, M. One-Dimensional Aggregation of Regioregular Polyalkylthiophenes. *Nano Lett.* **2003**, *3*, 707−712.
(17) Oh, J. Y.; Shin, M.; Lee, T. I.; Jang, W. S.; Min, Y.; Myoung, J. M.; Baik, H. K.; Jeong, U. Self-Seeded Growth of Poly(3-hexylthiophene) (P3HT) Nanofibrils by a Cycle of Cooling and Heating in Solutions. *Macromolecules* **2012**, *45*, 7504−7513.
(18) Son, H. J.; Carsten, B.; Jung, I. H.; Yu, L. P. Overcoming Efficiency Challenges in Organic Solar Cells: Rational Development of Conjugated Polymers. *Energy Environ. Sci.* **2012**, *5*, 8158−8170.
(19) Cheng, Y. J.; Yang, S. H.; Hsu, C. S. Synthesis of Conjugated Polymers for Organic Solar Cell Applications. *Chem. Rev.* **2009**, *109*, 5868−5923.
(20) Chang, M.; Lee, J.; Kleinhenz, N.; Fu, B. Y.; Reichmanis, E. Photoinduced Anisotropic Supramolecular Assembly and Enhanced Charge Transport of Poly(3-hexylthiophene) Thin Films. *Adv. Funct. Mater.* **2014**, *24*, 4457−4465.
(21) Zhao, K.; Xue, L. J.; Liu, J. G.; Gao, X.; Wu, S. P.; Han, Y. C.; Geng, Y. H. A New Method to Improve Poly(3-hexylthiophene) (P3HT) Crystalline Behavior: Decreasing Chains Entanglement to Promote Order-Disorder Transformation in Solution. *Langmuir* **2010**, *26*, 471−477.
(22) Kline, R. J.; McGehee, M. D.; Kadnikova, E. N.; Liu, J. S.; Frechet, J. M. J. Controlling the Field-Effect Mobility of Regioregular Polythiophene by Changing the Molecular Weight. *Adv. Mater.* **2003**, *15*, 1519−1522.
(23) Aiyar, A. R.; Hong, J. I.; Reichmanis, E. Regioregularity and Intrachain Ordering: Impact on the Nanostructure and Charge Transport in Two-Dimensional Assemblies of Poly(3-hexylthiophene). *Chem. Mater.* **2012**, *24*, 2845−2853.
(24) Aiyar, A. R.; Hong, J. I.; Izumi, J.; Choi, D.; Kleinhenz, N.; Reichmanis, E. Ultrasound-Induced Ordering in Poly(3-hexylthiophene): Role of Molecular and Process Parameters on Morphology and Charge Transport. *ACS Appl. Mater. Interfaces* **2013**, *5*, 2368−2377.
(25) Chang, M.; Lee, J.; Chu, P.-H.; Choi, D.; Park, B.; Reichmanis, E. Anisotropic Assembly of Conjugated Polymer Nanocrystallites for Enhanced Charge Transport. *ACS Appl. Mater. Interfaces* **2014**, *6*, 21541−21549.
(26) Choi, D.; Chang, M.; Reichmanis, E. Controlled Assembly of Poly(3-hexylthiophene): Managing the Disorder to Order Transition on the Nano-through Meso-Scales. *Adv. Funct. Mater.* **2015**, *25*, 920−927.
(27) Jaczewska, J.; Budkowski, A.; Bernasik, A.; Moons, E.; Rysz, J. Polymer vs Solvent Diagram of Film Structures Formed in Spin-Cast Poly(3-alkylthiophene) Blends. *Macromolecules* **2008**, *41*, 4802−4810.
(28) Xu, Y. Z.; Liu, J. G.; Wang, H. Y.; Han, Y. C. Hierarchical Network-Like Structure of Poly(3-hexlthiophene) (P3HT) by Accelerating the Disentanglement of P3HT in a P3HT/PS (Polystyrene) Blend. *RSC Adv.* **2013**, *3*, 17195−17202.
(29) Kim, Y. H.; Spiegel, D.; Hotta, S.; Heeger, A. J. Photoexcitation and Doping Studies of Poly(3-hexylthienylene). *Phys. Rev. B* **1988**, *38*, 5490−5495.
(30) Qiu, L. Z.; Wang, X.; Lee, W. H.; Lim, J. A.; Kim, J. S.; Kwak, D.; Cho, K. Organic Thin-Film Transistors Based on Blends of Poly(3-hexylthiophene) and Polystyrene with a Solubility-Induced Low Percolation Threshold. *Chem. Mater.* **2009**, *21*, 4380−4386.
(31) Yan, F.; Yu, S. M.; Zhang, X. W.; Qiu, L. H.; Chu, F. Q.; You, J. B.; Lu, J. M. Enhanced Proton Conduction in Polymer Electrolyte Membranes as Synthesized by Polymerization of Protic Ionic Liquid-Based Microemulsions. *Chem. Mater.* **2009**, *21*, 1480−1484.
(32) Lee, W. H.; Park, Y. D. Organic Semiconductor/Insulator Polymer Blends for High-Performance Organic Transistors. *Polymers* **2014**, *6*, 1057−1073.
(33) Emerson, J. A.; Toolan, D. T. W.; Howse, J. R.; Furst, E. M.; Epps, T. H. Determination of Solvent-Polymer and Polymer-Polymer Flory-Huggins Interaction Parameters for Poly(3-hexylthiophene) via Solvent Vapor Swelling. *Macromolecules* **2013**, *46*, 6533−6540.
(34) Heriot, S. Y.; Jones, R. A. L. An Interfacial Instability in a Transient Wetting Layer Leads to Lateral Phase Separation in Thin Spin-Cast Polymer-Blend Films. *Nat. Mater.* **2005**, *4*, 782−786.
(35) Tanaka, K.; Takahara, A.; Kajiyama, T. Film Thickness Dependence of the Surface Structure of Immiscible Polystyrene/Poly(methyl methacrylate) Blends. *Macromolecules* **1996**, *29*, 3232−3239.

DOI: 10.1021/acsami.5b03310
ACS Appl. Mater. Interfaces 2015, 7, 14095−14103

(36) Jaczewska, J.; Raptis, I.; Budkowski, A.; Goustouridis, D.; Raczkowska, J.; Sanopoulou, A.; Pamula, E.; Bernasik, A.; Rysz, J. Swelling of Poly(3-alkylthiophene) Films Exposed to Solvent Vapors and Humidity: Evaluation of Solubility Parameters. *Synth. Met.* **2007**, *157*, 726−732.
(37) Walheim, S.; Boltau, M.; Mlynek, J.; Krausch, G.; Steiner, U. Structure Formation via Polymer Demixing in Spin-Cast Films. *Macromolecules* **1997**, *30*, 4995−5003.
(38) Clark, J.; Chang, J. F.; Spano, F. C.; Friend, R. H.; Silva, C. Determining Exciton Bandwidth and Film Microstructure in Polythiophene Films Using Linear Absorption Spectroscopy. *Appl. Phys. Lett.* **2009**, *94*, 163303.
(39) Zhao, K.; Khan, H. U.; Li, R. P.; Su, Y. S.; Amassian, A. Entanglement of Conjugated Polymer Chains Influences Molecular Self-Assembly and Carrier Transport. *Adv. Funct. Mater.* **2013**, *23*, 6024−6035.
(40) Sun, G. X.; Chen, G. M.; Liu, J.; Yang, J. P.; Xie, J. Y.; Liu, Z. P.; Li, R.; Li, X. A Facile Gemini Surfactant-Improved Dispersion of Carbon Nanotubes in Polystyrene. *Polymer* **2009**, *50*, 5787−5793.
(41) Chua, L. L.; Zaumseil, J.; Chang, J. F.; Ou, E. C. W.; Ho, P. K. H.; Sirringhaus, H.; Friend, R. H. General Observation of *n*-Type Field-Effect Behaviour in Organic Semiconductors. *Nature* **2005**, *434*, 194−199.
(42) Wu, P. T.; Xin, H.; Kim, F. S.; Ren, G. Q.; Jenekhe, S. A. Regioregular Poly(3-pentylthiophene): Synthesis, Self-Assembly of Nanowires, High-Mobility Field-Effect Transistors, and Efficient Photovoltaic Cells. *Macromolecules* **2009**, *42*, 8817−8826.
(43) Chabinyc, M. L.; Street, R. A.; Northrup, J. E. Effects of Molecular Oxygen and Ozone on Polythiophene-Based Thin-Film Transistors. *Appl. Phys. Lett.* **2007**, *90*, 123508.

DOI: 10.1021/acsami.5b03310
ACS Appl. Mater. Interfaces 2015, 7, 14095−14103